Electronic Supplementary Information (ESI) available

In situ fabrication of porous $MnCo_xO_y$ nanocubes on Ti mesh as high performance monolith de-NO_x catalysts

Jing Xu,‡ Hongrui Li,‡ Yan Liu, Lei Huang, Jianping Zhang, Liyi Shi and Dengsong Zhang*

Research Center of Nano Science and Technology, School of Material Science and Engineering, Shanghai University, Shanghai 200444, China.

E-mail: dszhang@shu.edu.cn; Fax: +86-21-66136079; Tel: +86-21-66137152

‡ These authors contributed equally to this work

Supplementary experimental results

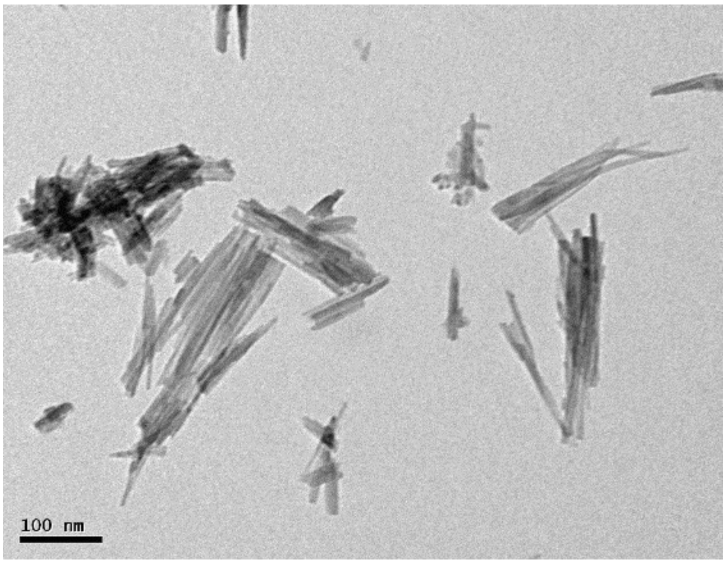

Fig. S1 TEM image of $MnCo_xO_y$ without Ti wire mesh.

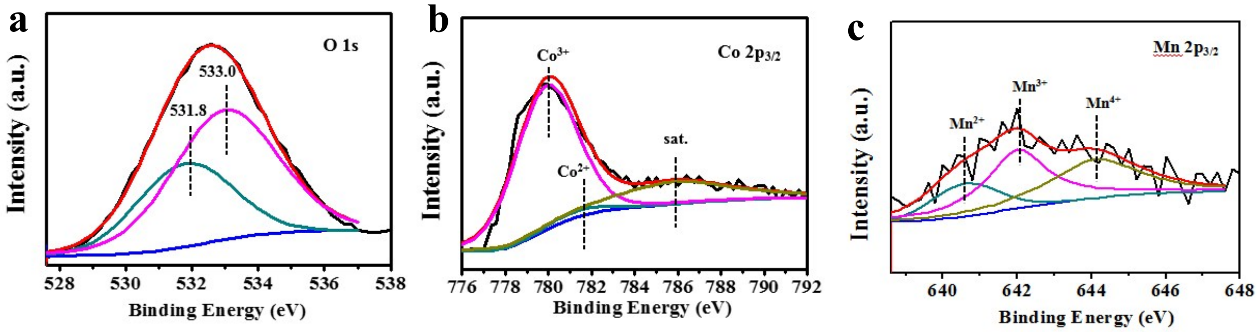

Fig. S2 XPS spectra for O 1s (a), Co 2p (b), and Mn 2p (c) of the catalyst

The X-ray photoelectron spectroscopy (XPS) were recorded on a Perkin–Elmer PHI 5000C ESCA system equipped with a dual X-ray source, using the Mg Kα (1253.6 eV) anode and a hemispherical energy analyzer. The background pressure during data acquisition was kept below 10^{-6} Pa. All binding energies were calibrated using contaminant carbon (C1s = 284.6 eV) as a reference.

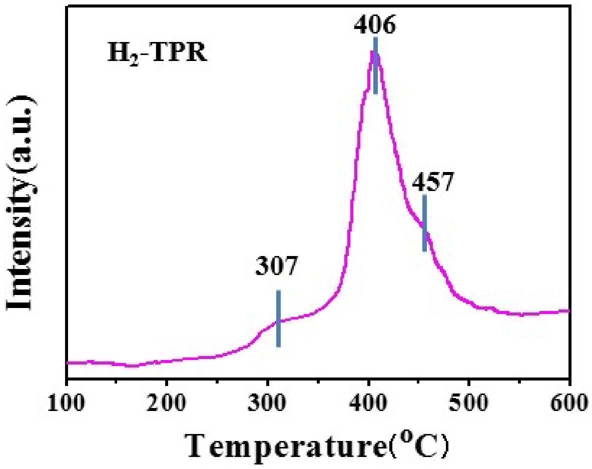

Fig. S3 H_2-TPR profile of the catalyst.

Temperature-programmed reduction by hydrogen (H_2-TPR) was carried out on a Tianjin XQ TP5080 auto-adsorption apparatus. Before the reduction process, the catalyst was outgassed at 300 °C under N_2 flow for 30 min and then cooled down to room temperature. Afterwards, the reactor temperature was raised to 600 °C at a constant heating rate of 10 $^{o}C \cdot min^{-1}$ in H_2 (5 vol. %)/N_2 with a flow rate of 30 $mL \cdot min^{-1}$ and the H_2 consumption data was recorded by a thermal conductivity detector (TCD).

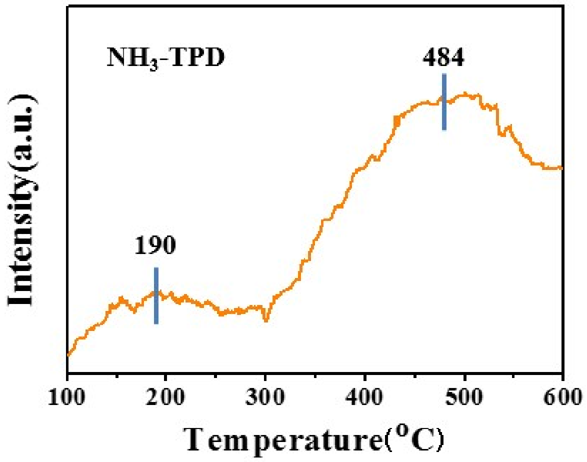

Fig. S4 NH_3-TPD profile of the catalyst

Temperature-programmed desorption experiments of ammonia (NH_3-TPD) were performed on the same Tianjin XQ TP5080 auto-adsorption apparatus and the desorption amounts of NH_3 was also monitored by the TCD. Prior to the experiments, the catalyst was pretreated at 300 ^{o}C in a flow of He (30 mL·min^{-1}) for 0.5 h and then cooled to 100 ^{o}C (under He protection). Subsequently, the samples were exposed to high purity anhydrous ammonia at 100 ^{o}C for 90 min, followed by He purging for 1h. Finally, the temperature was raised from 100 to 600 ^{o}C in He flow at a ramping rate of 10 ^{o}C·min^{-1}.

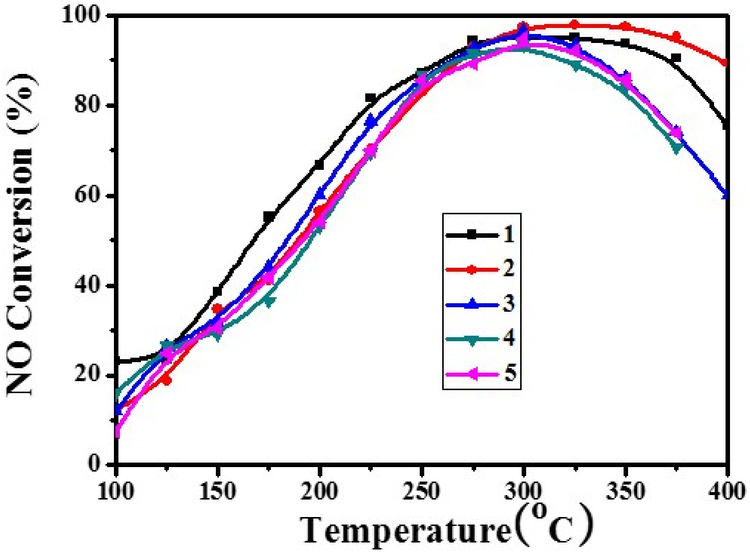

Fig. S5 NH_3-SCR performance of $MnCo_xO_y$@TiO_2@Ti wire mesh for five recyclable tests. Conditions: [NO] = [NH_3] = 500 ppm, [O_2] = 3 vol. %, N_2 as balance gas, and GHSV = 10,000 h^{-1}.

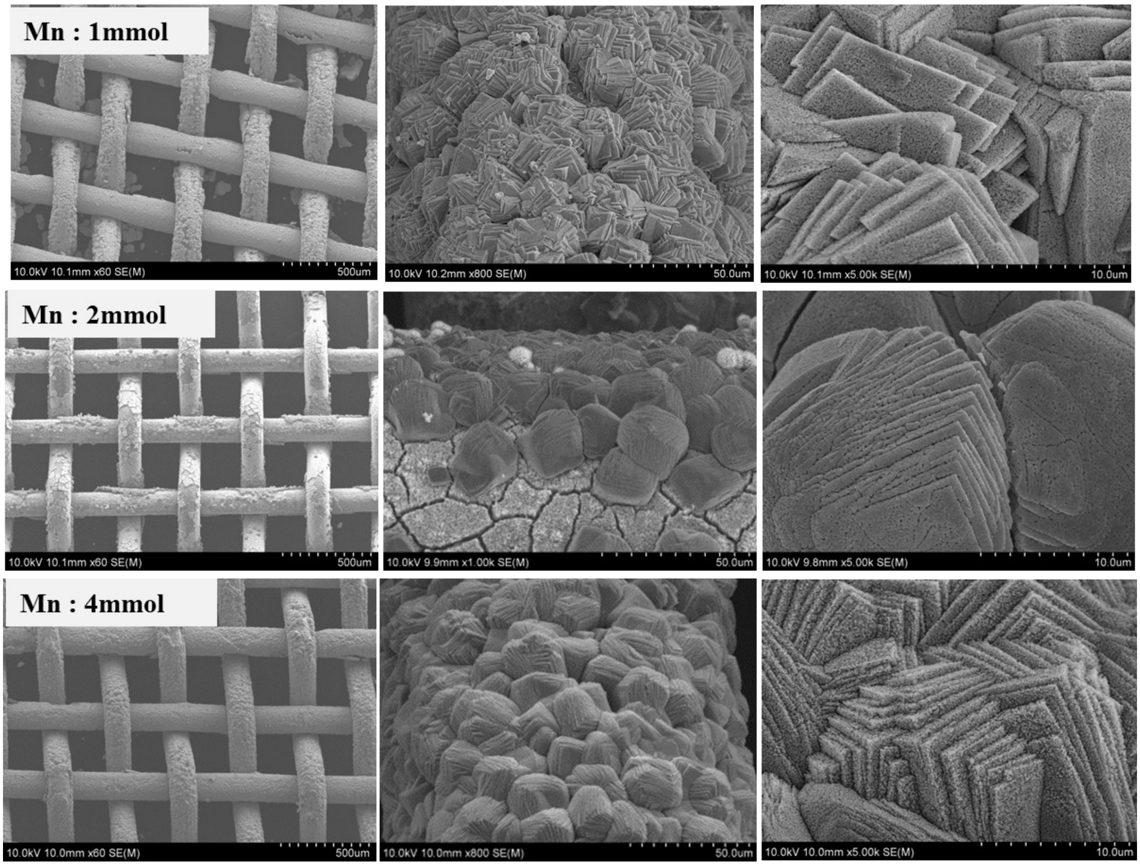

Fig. S6 SEM images of $MnCo_xO_y@TiO_2@Ti$ wire mesh prepared with different precursor concentrations.

Fig. S6 shows the SEM pictures of different solution concentrations of $MnCo_xO_y@TiO_2@Ti$ wire mesh. The active component on the surface of the titanium wire mesh is uniform loaded and presents the stacking structure of the three-dimensional layered nano cube. The nano cube is formed by stacking a porous sheet layer, and the whole titanium mesh surface is composed of a three-dimensional hierarchical ordered structure. With the change of solution concentration, the morphology is different. When the molar amount of Mn is 4mmol, the load of the surface active component on the titanium wire mesh is maximum and the layered cubic structure is the most regular and has the most exposed surface, which is useful to the adsorption and activation of the gas molecules in the process of denitrification and improve the catalyst activity.

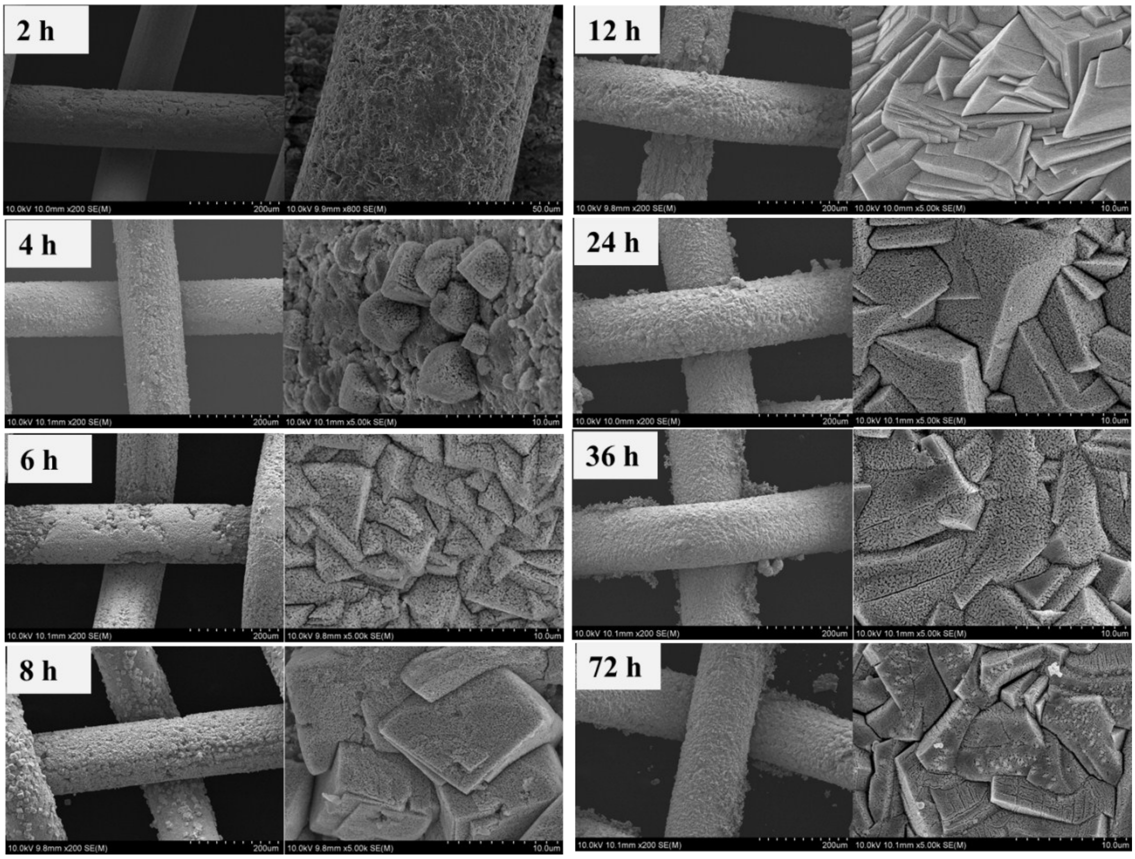

Fig. S7 SEM images of $MnCo_xO_y@TiO_2@Ti$ wire mesh wire mesh prepared with different reaction time.

In order to understand the growth of the active component on the surface of titanium mesh, The morphology of as-prepared $MnCo_xO_y@TiO_2@Ti$ wire mesh with different reaction time was investigated by means of scanning electron microscopy (SEM). Fig. S7 shows morphology under different magnification. After 2 h of hydrothermal reaction, there are almost no active components on the TiO_2 surface. With the extension of the hydrothermal time, the active load gradually increased and evenly loaded on the surface. They reached the saturated load at 12 h and loading without too big change to prolong the hydrothermal time. The excess activity of group division growth of stacked on the existing structure. As can be seen from the SEM images of high resolution, with the extension of hydrothermal reaction, manganese and cobalt ion deposition on the surface of titanium mesh, nucleation, grain formation and gradually grow. After calcined form with an array of three-dimensional hierarchical porous nanocubes, they evenly coated on the surface of titanium mesh and form a stable morphology structure after 12h. The structure does not change with the increase of the reaction time.

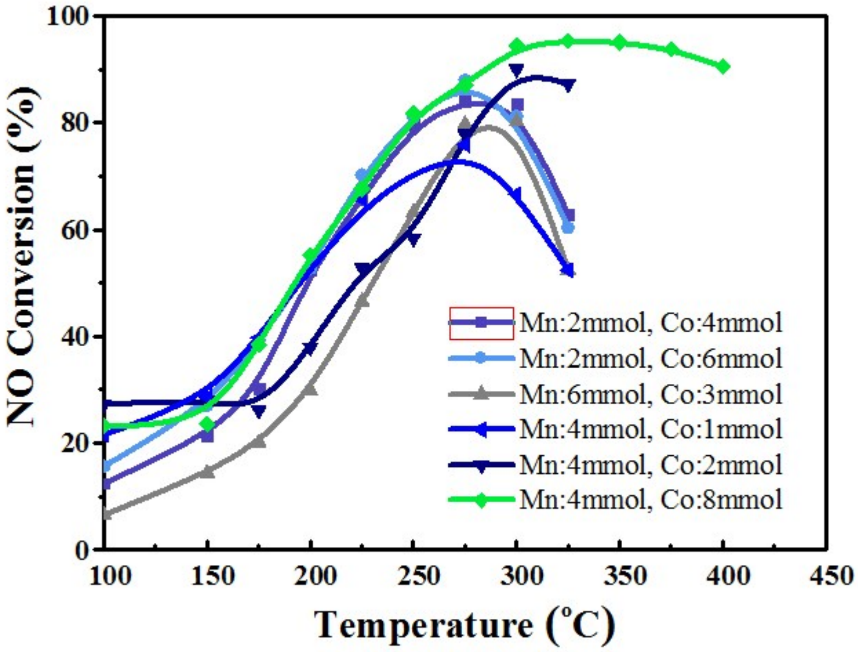

Fig. S8 Plots of NO conversion versus temperature for wire mesh $MnCo_xO_y@TiO_2@Ti$ with different molar quantities of Mn and Co.

The effect of different addition of Mn and Co on the performance of catalysts has been shown in Fig. S8. For the monolithic catalyst, the amount of active component loaded on the surface of titanium mesh was related to the molar amount of manganese and cobalt in the precursor salt solution. Therefore, by adjusting the molar amount of manganese and cobalt in the solution, the load capacity of the surface active component of the titanium wire mesh can be adjusted, which directly influence the SCR performance of the catalyst. When the concentration of $MnSO_4·H_2O$ was 4 mmol and $Co (NO_3)_2·6H_2O$ was 8 mmol, the catalyst has the best catalytic activity in the entire temperature range compared to the other catalysts. In the temperature range of 275~400 ^oC, the NO conversion rate is more than 87% and reached a maximum value of 96% at 325 ^oC.

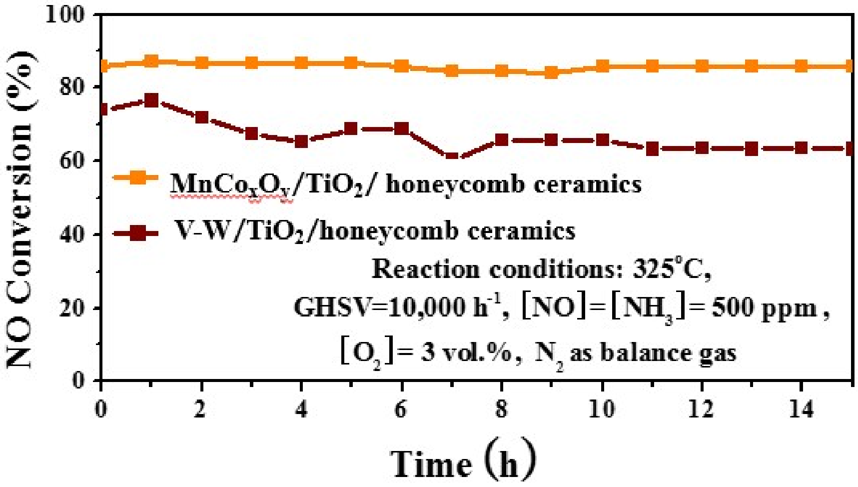

Fig. S9 Stability test at 325 °C for 15 h of $MnCo_xO_y/TiO_2$/ honeycomb ceramics and V-W/TiO_2/honeycomb ceramics.

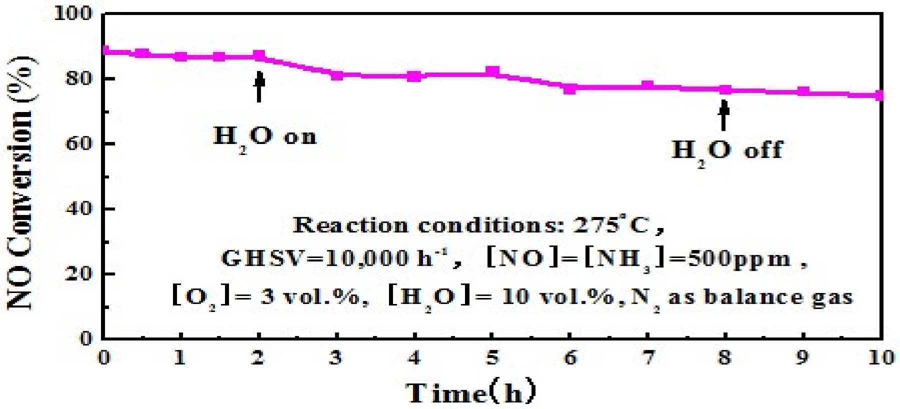

Fig. S10 H_2O durability test of the $MnCo_xO_y$@TiO_2 @Ti wire mesh at 275◦C.

The NO conversion of the catalyst was about 90% when it was not in steam. After the introduction of 10 vol. % H_2O at 275°C, the conversion rate slow down to 80% during the 6h test. The present of water vapor and NH_3 molecules on the surface of the catalyst activity compete for adsorption sites made to inhibit the reactive gas molecules adsorption and activation. However, after removing H_2O, the conversion of NO remained unchanged.

Table S1 Performance of various catalysts for SCR of NO with NH_3

Catalyst	Feed composition			t (°C)	X (%)	GHSV (h^{-1})
	NO (ppm)	NH_3 (ppm)	O_2 (%)			
$MnCo_xO_y$@TiO_2 @Ti	500	500	3	275	92	10,000
$Mn_xCo_{3-x}O_4$ [26]	500	500	3	150	98	38,000
Mn-Ce/TiO_2 [8]	800	800	3	150	89	40,000
MnO_x/TiO_2 [4]	500	500	2	250	88	60,000